Polarization of Light

PHY324, February 19 2023

Emre Alca 1005756193, Jace Alloway 1006940802

Abstract

Lorem ipsum dolor sit amet, consectetuer adipiscing elit. Ut purus elit, vestibulum ut, placerat ac, adipiscing vitae, felis. Curabitur dictum gravida mauris. Nam arcu libero, nonummy eget, consectetuer id, vulputate a, magna. Donec vehicula augue eu neque. Pellentesque habitant morbi tristique senectus et netus et malesuada fames ac turpis egestas. Mauris ut leo. Cras viverra metus rhoncus sem. Nulla et lectus vestibulum urna fringilla ultrices. Phasellus eu tellus sit amet tortor gravida placerat. Integer sapien est, iaculis in, pretium quis, viverra ac, nunc. Praesent eget sem vel leo ultrices bibendum. Aenean faucibus. Morbi dolor nulla, malesuada eu, pulvinar at, mollis ac, nulla. Curabitur auctor semper nulla. Donec varius orci eget risus. Duis nibh mi, congue eu, accumsan eleifend, sagittis quis, diam. Duis eget orci sit amet orci dignissim rutrum.

Introduction

In introductory optics and electromagnetism, light polarization is the instrinsic property of electromagnetic waves which is given by the orientation of propogation. Generally, there are three types of light polarization: linear, circular, and elliptical. Most light is linearly polarized, and may be manually polarized by means of a polarizer, by reflection, scattering, or refraction through denser media.

Maxwell's equations predict the linear polarization of light as perpendicular electric and magnetic field components, which then are both perpendicular to the direction of the propogation. This allows various projections of these components on vertical and horizontal axes, hence polarizing the light. Any light passing through a polarizer is then polarized in the direction of the polarizer.

Today, polarizers are used in sunglasses, laser physics, photography, and other ranges of electromagnetic waves (radio, x-rays, gamma rays, etc).

Theory

In the absence of electric charge and current distributions, Maxell's equations may be rearranged and re-substituted to obtain the wave equations for typical electric and magnetic field components:

$$\Box^2 \mathbf{E}(\mathbf{r},t) = 0, \qquad \Box^2 \mathbf{B}(\mathbf{r},t) = 0, \tag{1}$$

where $\Box^2 \equiv \nabla^2 - \frac{1}{c^2}\frac{\partial^2}{\partial t^2}$ is the D'Alembertian operator. Solving these equations by D'Alembert's method provides expressions for $\mathbf{E}$ and $\mathbf{B}$ as

$$\mathbf{E}(\mathbf{r},t) = \text{Re}\left\{\boldsymbol{\mathcal{E}}_0 \exp\left(i\frac{\omega}{c}(\mathbf{n}\cdot\mathbf{r} - ct)\right)\right\} \tag{2.1}$$

$$\mathbf{B}(\mathbf{r},t) = \text{Re}\left\{\boldsymbol{\mathcal{B}}_0 \exp\left(i\frac{\omega}{c}(\mathbf{n}\cdot\mathbf{r} - ct)\right)\right\}, \tag{2.2}$$

where $\boldsymbol{\mathcal{E}}_0$ and $\boldsymbol{\mathcal{B}}_0$ are the electric and magnetic wave directions, respectively, ω is the angular frequency of the wave, and $\mathbf{n}$ the direction of propogation.

Then, (2.1) and (2.2) are related by Faraday's Law,

$$\nabla \times \mathbf{E} + \frac{\partial \mathbf{B}}{\partial t} = 0, \tag{3}$$

which yields the electro-magnetic wave relation

$$\text{Re}\left\{\left(i\frac{\omega}{c}\mathbf{n}\times\boldsymbol{\mathcal{E}}_0 - i\omega\boldsymbol{\mathcal{B}}_0 \exp\left(i\frac{\omega}{c}(\mathbf{n}\cdot\mathbf{r} - ct)\right)\right)\right\} = 0, \tag{4}$$

which is true for all space and time components. Therefore $\boldsymbol{\mathcal{B}}_0 = \frac{1}{c}\mathbf{n}\times\boldsymbol{\mathcal{E}}_0$, resulting in perpendicular electric and magnetic field components of a light wave. Polarization is the effect of projecting these vector components of (4) onto a plane, reducing the light intensity and specifying a polarized direction.

This report focuses on two interesting effects of light polarization: Malus's law, and reflectance polarization in the form of Brewster's angle. Malus's

law models the effects of polarizers aligned in series to each other, and how the intensity of the light changes.

In its simplist form, Malus's law states that the intensity of light as it passes through two polarizers is proportional to $\cos^2\theta$, where θ is the angle between the two polarizers. Suppose the polarizer is oriented in the $\hat{y}$ direction, and let the transmission axis of this second polarizer be $\hat{y}'$. In this case, the components of the wave which pass through this second polarizer is

$$E_{x'} = E\sin\theta \qquad\qquad E_{y'} = E\cos\theta \tag{5}$$

with the $\hat{y}'$ component being transmitted only (since $\hat{x}'$ is orthogonal to the transmission axis of the second polarizer). By definition, since intensity is proportional to the square of the electric field component, $I_0 = E^2$ (the intensity between the polarizers), thus the intensity of light transmitted by both of them is

$$I(\theta) = E^2\cos^2\theta = I_0\cos^2\theta \tag{6}$$

This expression is called Malus's Law. For this experiment, θ is known from our measurements, and $I(\theta)$ will be extrapolated using an optimization algorithm.

If a third polarizer is placed further along the $\hat{z}$ axis (after the polarizer and the analyzer) such that its transmission axis is orthoginal to that of the polarizer, some intensity does, interstingly, transmit through. The intensity that passes through this third polaroid can be found by applying Malus's law again. If the intensity of light passing through the polarizer is I_1, the the intensity through the analyzer is

$$I_2 = I_1\cos^2\varphi$$

where φ is the angle between the transmission axes of the polarizer and analyzer. Applying Malus's law for the second time yields

$$\begin{aligned} I_3 &= I_2\cos^2(\frac{\pi}{2}-\varphi) \\ &= I_1\cos^2(\varphi)\cos^2(\frac{\pi}{2}-\varphi)7) \qquad (() \\ &= \frac{I_1}{4}sin^2(2\varphi) \end{aligned}$$

Much like the expression for two polaroids, φ is known and I_1 must be extrapolated using an optimization program.

Methodology

Data Analysis

Following the form of the report, Malus's Law will be discussed first. The data, as recorded in *Labview*, was stored in separate .txt files for each of the two trials (2 and 3 polaroids). These files were read by the python library *numpy*'s *.readtxt*() function, and isolated by column for *Intensity* (V) and *position* (*radians*). he raw data was plotted using another python library, *matplotlib*, with uncertainties (see the upper charts of Figure N and Figure N+1 for the plots of the 2- and 3-polariod trials respectively). The uncertainties for each of these charts was one half of the smallest significant digit. The plot for 2-polarids was fit using an equation in the form of (6), and for 3-polaroids was fit using an equation in the form of (7) using *scipy.optimize.curve_fit*(). Each of these functions had additional parameters for a phase-shift and an intensity offset.

The function fit the 3-polaroid trial quite easily, but the 2-polaroid trial was a little bit more tricky. The flatter tails at either end of the sinusoidal wave were culled from the dataset, and the function was able to fit (see Figure N to see the comparison between the original and culled data).

The results of these fits are discussed in the *Results and Discussion section below*. The uncertainties of the relevant parameters of these fits (for these functions, I_0 and I_1 for the 2- and 3-polaroid trials respectively) were found by taking the square root of the covariance of the optimized parameters found by *scipy.optimize.curve_fit*. So long as the maximum value of the curve generated by these optimized parameters (as well as the majority of the curve itself) fit within the uncertainties of the measured data, the parameters are sufficient, within the uncertainty of the measurements. The residual plots of each trial (the difference between the fit curve and the measured data) were also plotted (the residual plots can be found in the lower charts of Figure N and Figure N+1).

Results and Discussion

The computed values for the thermal diffusivity m, along with the respective uncertainties, were extracted from the optimal curve_fit parameters. These values, along with the fitting data and χ^2 probabilities, are included in Table 1. The data was plotted,

including the applied temperature square wave (Figure 3). The uncertainty analysis, described previously, was then carried out and plotted in Figure 4.

These values were compared with an expected value for thermal diffusivity, taken from [1], which was $m = 0.95 \pm 0.17\,\text{mm}^2/\text{s}$, while another source [2] yielded
$m = 0.089 - 0.13\,\text{mm}^2/\text{s}$. Overall, in comparison to the results, a significant overlap from expected and computed values was noted, thus concluding a successful draw of results from the data.

Lastly, from examining results, a large difference in m was noted between the 120s and 90s trials. This was attributed to the 90s trial being too short of a time interval, hence yielding a value of m higher than expected due to the shorter amount of time for energy transfer, since this assumes a denser medium. From Figure 3, it is noticeable that the 90s trial (2) has a much smaller amplitude than that of the 120s trials (1 and 3). In the future, it is recommended to perform trials with longer periods and significant patience.

Conclusions

Overall, it was concluded that the thermal diffusivity of the rubber tube was within the range of the expected experimental value specified in literature for polypropylene. Despite difficulties such as tedious data collection, curve fitting, and uncertainty analysis, the results yielded were valid within the uncertainty range.

Bibliography

[1] Martínez, K., Marín, E., Glorieux, C., Lara-Bernal, A., Calderón, A., Rodríguez, G. P., & Ivanov, R. (2015). Thermal diffusivity measurements in solids by photothermal infrared radiometry: Influence of convection–radiation heat losses. International Journal of Thermal Sciences, 98, 202-207. https://doi.org/10.1016/j.ijthermalsci.2015.07.019

[2] Edge, E. (n.d.). Thermal diffusivity table. Engineers Edge - Engineering, Design and Manufacturing Solutions. Retrieved February 9, 2023, from https://www.engineersedge.com/heat_transfer/thermal_diffusivity_table_13953.htm

[3] Thermal Diffusivity of Tortured Rubber and Bessel Functions. University of Toronto Practicals, PHY324 Manual. https://www.physics.utoronto.ca/~phy224_324/experiments/thermal-diffusivity/labheat.pdf

Appendix I: Figures and Tables

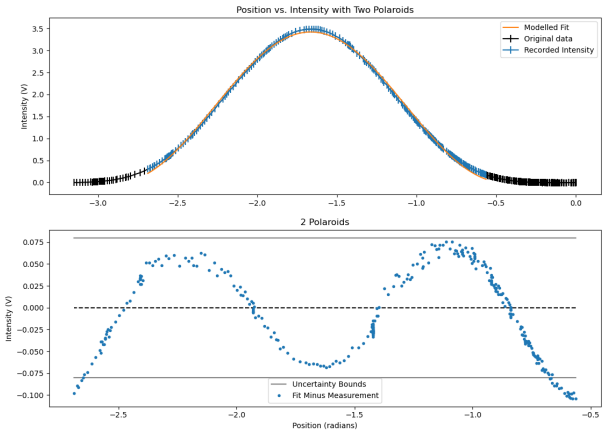

1: add later.

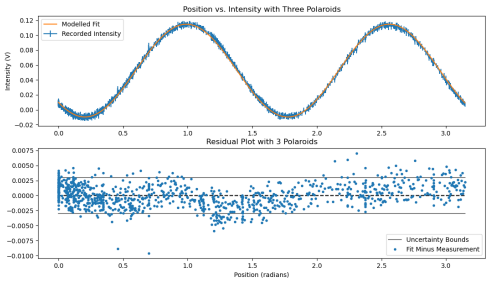

2: add later.

Trial	Period (s)
$m_1L_1\theta_1$	1.442±0.612
$m_1L_1\theta_2$	1.623±0.649
$m_1L_2\theta_1$	1.275±0.48
$m_1L_2\theta_2$	1.11±0.223
$m_2L_1\theta_1$	1.386±0.644
$m_2L_1\theta_2$	1.434±0.324
$m_2L_2\theta_1$	1.181±0.293
$m_2L_2\theta_2$	1.369±0.589

[Table 1] Results obtained for the computed values of the thermal diffusivity for each of the three trials. Included is the applied angular period, the intial temperature of the rubber, the curve_fit computed value for the thermal diffusivity and uncertainty, and the quality of the χ^2 fit.

Trial	τ (s^{-1})	χ^2 (probability)
$m_1L_2\theta_1$	166±2.1	0.2
$m_1L_2\theta_2$	334±12	0.3
$m_1L_2\theta_1$	86.5±49	0.0
$m_2L_2\theta_1$	26.9±6.9	0.0

[Table 1] Results obtained for the computed values of the thermal diffusivity for each of the three trials. Included is the applied angular period, the intial temperature of the rubber, the curve_fit computed value for the thermal diffusivity and uncertainty, and the quality of the χ^2 fit.